Aerosol composition and sources during the Chinese Spring Festival: fireworks, secondary aerosol, and holiday effects

Qi Jiang[1,3], Yele Sun[1,2*], Zifa Wang[1], Yan Yin[2,3]

[1]State Key Laboratory of Atmospheric Boundary Layer Physics and Atmospheric Chemistry, Institute of Atmospheric Physics, Chinese Academy of Sciences, Beijing 100029, China

[2]Collaborative Innovation Center on Forecast and Evaluation of Meteorological Disasters, Nanjing University of Information Science & Technology, Nanjing, 210044, China

[3]Key Laboratory for Aerosol-Cloud-Precipitation of China Meteorological Administration, Nanjing University of Information Science & Technology, Nanjing 210044, China

Correspondence to: sunyele@mail.iap.ac.cn

Abstract

Aerosol particles were characterized by an Aerodyne Aerosol Chemical Speciation Monitor along with various collocated instruments in Beijing, China to investigate the roles of fireworks (FW) and secondary aerosol in particulate pollution during the Chinese Spring Festival of 2013. Three fireworks events exerting significant and short-term impacts on fine particles ($PM_{2.5}$) were observed on the days of Lunar New Year, Lunar Fifth Day, and Lantern Festival. The FW showed large impacts on non-refractory potassium, chloride, sulfate, and organics in submicron aerosol (PM_1), of which the FW organics appeared to be emitted mainly in secondary with its mass spectrum resembling to that of secondary organic aerosol (SOA). Pollution events (PEs) and clean periods (CPs) alternated routinely throughout the study. Secondary particulate matter (SPM = SOA + sulfate + nitrate + ammonium) dominated the total PM_1 mass on average accounting for 63-82% during nine PEs in this study. The elevated contributions of secondary species during PEs resulted in a higher mass extinction efficiency of PM_1 (6.4 $m^2 g^{-1}$) than that during CPs (4.4 $m^2 g^{-1}$). The Chinese Spring Festival also provides a unique opportunity to study the impacts of reduced anthropogenic emissions on aerosol chemistry in the city. The primary species showed ubiquitous reductions during the holiday period with the largest reduction for cooking OA (69%), nitrogen monoxide (54%), and coal combustion OA (28%). The secondary sulfate, however, remained minor change, and the SOA and the total $PM_{2.5}$ even slightly increased. Our results have significant implications that controlling local primary source emissions during PEs, e.g., cooking and traffic activities, might have limited effects on improving air quality in megacity Beijing due to the dominance of SPM from regional transport in aerosol particle composition.

1 Introduction

Air pollution caused by fine particles ($PM_{2.5}$) is of great concern in densely populated megacities because of its adverse effects on human health and regional air quality (Molina and Molina, 2004; Chan and Yao, 2008). The health risk of air pollution is greater than expected leading to around 7 million people's death in 2012 according to the latest report by World Health Organization (http://www.who.int/mediacentre/news/releases/2014/air-pollution/en/). The Beijing metropolitan area is one of the most populous megacities in the world with the population reaching 20.69 million by the end of 2012 (Beijing Municipal Bureau of Statistics). According to Beijing Municipal Environmental Protection Bureau, the annual average concentration of $PM_{2.5}$ was 89.5 μg m^{-3} in 2013, which is about 2.5 times the National Ambient Air Quality Standards of China (35 μg m^{-3} for annual average). This suggests severe fine particle pollution in Beijing. Extensive studies have been made recently to investigate the chemical composition and sources of $PM_{2.5}$. The results showed that secondary inorganic aerosol (SIA = sulfate + nitrate + ammonium), coal combustion, traffic emissions (gasoline and diesel), biomass burning, cooking emissions and dust are the major sources of $PM_{2.5}$ (Zheng et al., 2005; Song et al., 2006; Zhang et al., 2013). However, the source contributions varied significantly among different seasons, therefore improving air quality in Beijing remains a great challenge due to the very complex sources and dynamic evolution processes of aerosol particles.

Fine particles from various sources can be either primary from direct emissions, e.g., fossil fuel combustion and biomass burning, or secondary from atmospheric oxidation of gas-phase species. The fireworks (FW) is one of the most important

primary sources that can exert significant and short-time impacts on air quality. The fireworks burning emits a large amount of gaseous pollutants, e.g., sulfur dioxide (SO_2) and nitrogen oxide (NO_x) (Vecchi et al., 2008; Huang et al., 2012), and also fine particles comprising organic/elemental carbon, sulfate, potassium, chloride and various metals, e.g., copper (Cu), barium (Ba), strontium (Sr) and magnesium (Mg) (Moreno et al., 2007; Wang et al., 2007; Li et al., 2013). The enhanced short-term air pollution by fireworks can substantially increase health risk levels (Godri et al., 2010; Yang et al., 2014) and reduce visibility for hours (Vecchi et al., 2008). Previous studies on chemical characterization of fireworks in China were mostly based on filter measurements with a time resolution of 12 h or 24 h (Wang et al., 2007; Zhang et al., 2010; Feng et al., 2012; Huang et al., 2012; Cheng et al., 2014; Zhao et al., 2014). Considering that the fireworks events usually last less than 12 hours, the filter analysis may introduce large uncertainties in accurate quantification of chemical composition of FW particles due to either the interferences of non-FW (NFW) background aerosols or the difficulties to account for meteorological variations. Drewnick et al. (2006) first conducted real-time size-resolved chemical composition measurements during the New Year's period in Mainz, Germany using an Aerodyne Time-of-Flight Aerosol Mass Spectrometer (ToF-AMS). To our knowledge, there are no such real-time measurements of chemical composition of aerosol particles during fireworks events in China yet, which limits our understanding on the rapid formation and evolution of fireworks events, and also their impacts on particulate matter (PM) pollution.

Secondary aerosol is of more concern compared to primary aerosol because it is formed over regional scales and exerts impacts on air quality over wider areas (Matsui

et al., 2009; DeCarlo et al., 2010). Therefore, extensive studies have been conducted in recent years to characterize the sources and formation mechanisms of secondary aerosol (Yao et al., 2002; Duan et al., 2006; Sun et al., 2006; Wang et al., 2006; Guo et al., 2010; Yang et al., 2011; Sun et al., 2013b; Zhang et al., 2013; Zhao et al., 2013). SIA was observed to contribute a large fraction of $PM_{2.5}$ and played an enhanced role during haze episodes due to the faster heterogeneous reactions associated with higher humidity (Liu et al., 2013; Sun et al., 2013a; Zhao et al., 2013; Sun et al., 2014; Wang et al., 2014). While SIA was relatively well characterized, secondary organic aerosol (SOA) is not well understood (Huang et al., 2014). The recent deployments of Aerodyne Aerosol Mass Spectrometers (AMS) greatly improved our understanding on sources and evolution processes of organic aerosol (OA) in China, and also the different roles of primary organic aerosol (POA) and SOA in PM pollution (Huang et al., 2010; Sun et al., 2010; He et al., 2011; Sun et al., 2012; Sun et al., 2013b; Zhang et al., 2014). While SOA is more significant in summer (Huang et al., 2010; Sun et al., 2010; Sun et al., 2012), POA generally plays a more important role during wintertime (Sun et al., 2013b). Recently, the role of SOA in fine particle pollution during wintertime – a season with frequent occurrences of pollution episodes in Beijing was extensively investigated and the results highlighted the similar importance of SOA to SIA (Sun et al., 2013b; Sun et al., 2014; Zhang et al., 2014). However, the role of SOA in particulate pollution during periods with largely reduced anthropogenic activities is not well known yet (Huang et al., 2012). This study happened to take place in a month with the most important holiday in China, i.e., the Spring Festival. The source emissions (e.g., traffic and cooking) have significant changes due to a large reduction of population and anthropogenic activities in the city. This provides a unique opportunity to investigate how source changes affect aerosol chemistry

115 including primary emissions and secondary formation in Beijing. Although Huang et
116 al. (2012) investigated such a holiday effect on aerosol composition and optical
117 properties in Shanghai, the data analyses were limited by daily average composition
118 measurements and also the significantly different meteorological conditions between
119 holiday and non-holiday periods.

120 In this study, an Aerosol Chemical Speciation Monitor (ACSM) along with
121 various collocated instruments was deployed in Beijing during February 2013. The
122 chemical composition of submicron aerosol (PM_1) from fireworks is quantified based
123 on the highly time – resolved measurements of non-refractory submicron aerosol
124 (NR-PM_1) species (organics, sulfate, nitrate, ammonium, chloride, and potassium) and
125 black carbon. The impacts of fireworks on PM pollution during Chinese Lunar New
126 Year (LNY), Lunar Fifth Day (LFD), and Lantern Festival (LF) are investigated, and
127 the roles of secondary formation in PM pollution are elucidated. Further, the effects of
128 reduced anthropogenic emissions on primary and secondary aerosols in the city are
129 illustrated, which has significant implications for making air pollution control
130 strategies in Beijing.

131 ## 2 Experimental method

132 ### 2.1 Sampling site

133 The measurements in this study were conducted at the Institute of Atmospheric
134 Physics (IAP), Chinese Academy of Sciences (39°58'28''N, 116°22'16"E), an urban
135 site located between the north third and fourth ring road in Beijing (Sun et al., 2012).
136 Aerosol measurements were performed from 1 February to 1 March 2013 when three
137 episodes with significant influences of fireworks, i.e., Lunar New Year (LNY), Lunar
138 Fifth Day (LFD), and Lantern Festival (LF), were observed (Fig. 1). The

meteorological conditions during the measurement period are reported in Fig. 1. Winds at the ground surface were generally below 2 m s^{-1} and temperature averaged 0.6 °C. Relative humidity (RH) varied periodically with higher values generally associated with higher PM pollution.

2.2 Aerosol sampling

The chemical composition of NR-PM_1 including organics, sulfate, nitrate, ammonium, and chloride were measured *in situ* by the ACSM at an approximate 15-min time intervals (Ng et al., 2011b). The ACSM has been widely used for long-term and routine aerosol particle composition measurements due to its robustness (Sun et al., 2012; Budisulistiorini et al., 2014; Petit et al., 2014) despite its lower sensitivity and mass resolution compared to previous versions of research-grade AMS (Jayne et al., 2000; DeCarlo et al., 2006). . In this study, the ambient air was drawn inside the sampling room at a flow rate of 3 L min^{-1}, of which ~0.1 L min^{-1} was sub-sampled into the ACSM and 0.85 L min^{-1} into a Cavity Attenuated Phase Shift Spectrometer (CAPS) particle extinction monitor (Massoli et al., 2010). A $PM_{2.5}$ cyclone (Model: URG-2000-30ED) was supplied in front of the sampling line to remove coarse particles with aerodynamic diameters larger than 2.5 μm. The aerosol particles were dried by a silica gel dryer (RH < 40%) before entering the ACSM and the CAPS. The ACSM was operated at a scan rate of 500 ms amu^{-1} for the mass spectrometer from *m/z* 10 – 150. Because ACSM cannot detect refractory components, e.g., BC and mineral dust, a two-wavelength Aethalometer (Model AE22, Magee Scientific Corp.) was therefore used to measure refractory BC in $PM_{2.5}$. The light extinction of dry fine particles (b_{ext}, 630 nm) was measured at 1 s time resolution with a precision (3 σ) of 1 M m^{-1} by the CAPS monitor. In addition, the mass concentration

of $PM_{2.5}$ was determined by a heated Tapered Element Oscillating Microbalance, TEOM, and the collocated gaseous species (including CO, SO_2, NO, NO_x and O_3) were measured by various gas analyzers (Thermo Scientific) at 1 min time resolution. A more detailed descriptions of aerosol and gas measurements were given in Sun et al. (2013b).

2.3 ACSM data analysis

The ACSM data were analyzed for the mass concentrations and chemical composition of NR-PM_1 using standard ACSM software (v 1.5.3.2) written within Igor Pro (WaveMetrics, Inc., Oregon USA). A composition-dependent collection efficiency (CE) recommended by Middlebrook et al.(2012), CE = max (0.45, 0.0833 + 0.9167 × ANMF), was used to account for the incomplete detection due to the particle bouncing effects (Matthew et al., 2008) and the influences caused by high mass fraction of ammonium nitrate (ANMF). Because aerosol particles were overall neutralized ($NH_4^+{}_{measured}/NH_4^+{}_{predicted}$ = 1.01, r^2 = 0.99) and also dried before entering the ACSM, the effects of particle acidity and RH would be minor (Matthew et al., 2008; Middlebrook et al., 2012). The default relative ionization efficiencies (RIEs) except ammonium (RIE = 6.5) that was determined from the IE calibration were used in this study..Quantification of K^+ is challenging for ACSM because of a large interference of organic $C_3H_3^+$ at *m/z* 39 and also uncertainties caused by surface ionization (Slowik et al., 2010). In this work, we found that *m/z* 39 was tightly correlated with *m/z* 43 that is completely organics during non-fireworks (NFW) periods (r^2 = 0.87, slope = 0.45, Fig. S1). However, higher ratios of *m/z* 39/43 during FW periods were observed due to the elevated K^+ signal from burning of fireworks. Assuming that *m/z* 39 was primarily contributed by organics during NFW periods, the

187 excess *m/z* 39 signal, i.e., K^+, can then be estimated as *m/z* 39 – *m/z* 43 × 0.45. The
188 $^{41}K^+$ at *m/z* 41 was calculated using an isotopic ratio of 0.0722, i.e., $^{41}K^+ = 0.0722 \times$
189 K^+. The K^+ signal was converted to mass concentration with a RIE of 2.9 that was
190 reported by Drewnick et al. (2006). It should be noted that the quantification of K^+ in
191 this study might have a large uncertainty because of the unknown RIE of K^+ (RIE_K).
192 The RIE_K can vary a lot depending on the tuning of the spectrometer and the
193 temperature of the vaporizer. For example, Slowik et al. (2010) reported a $RIE_K = 10$
194 based on the calibration of pure KNO_3 particles using a ToF-AMS, which is much
195 higher than the $RIE_K = 2.9$ obtained from the comparisons of K/S from fireworks and
196 AMS measurements (Drewnick et al., 2006). In addition, the stability of surface
197 ionization (SI) and electron impact (EI) also affects RIE_K. We then checked the
198 variations of the ratio of *m/z* 39/*m/z* 23 (two *m/z*'s with similar surface ionization
199 issues). The average ratio of *m/z* 39/23 during LFD and LF is 8.7 and 11.1,
200 respectively, which is close to 9.0 during the NFW periods. The results suggest that
201 the SI/EI ratio was relatively stable throughout the study. Because we didn't have
202 collocated K measurement, $RIE_K = 2.9$ that was estimated from fireworks was used in
203 this study. The quantified K^+ during LFD and LF on average contributed 4.5% and
204 4.7% of PM_1, respectively, which is close to ~5% ($PM_{2.5}$) reported by Cheng et al.
205 (2014). Also, the large contribution of K^+ to PM_1 (20.5%) during LNY, likely due to
206 the intensified firework emissions (mainly firecrackers), is consistent with that (17.3%)
207 observed during LNY 2014 in megacity Tianjin (Tian et al., 2014). Using RIE_K=10
208 will decrease the K^+ concentration by a factor of more than 3, which appears to
209 underestimate K^+ a lot. Therefore, $RIE_K = 2.9$ for the quantification of K^+ in our study
210 appear to be reasonable. The KCl^+ (*m/z* 74) and $^{41}KCl^+/K^{37}Cl^+$ (*m/z* 76) were
211 estimated by the differences between the measured and PMF modeled *m/z* 74 (Fig.

S2). Not surprisingly, the quantified KCl^+ highly correlates with K^+ ($r^2 = 0.82$, Fig. S2c). The chloride concentration was also biased at *m/z* 35 during some periods (e.g., LNY, Fig. S3), which is likely due to the interferences of NaCl from fireworks. Therefore, Cl^+ (*m/z* 35) was recalculated based on its correlation with *m/z* 36 (mainly HCl^+ with negligible C_3^+ and ^{36}Ar), i.e., *m/z* 35 = 0.15 × *m/z* 36. The $^{37}Cl^+$ was calculated using an isotopic ratio of 0.323, i.e., $^{37}Cl^+ = 0.323 \times {}^{35}Cl^+$. The comparison of the reconstructed chloride from the default values is shown in Fig. S3b.

The positive matrix factorization (PMF) with the algorithm of PMF2.exe in robust mode (Paatero and Tapper, 1994) was performed on organic aerosol (OA) mass spectra (*m/z* 12 – 120) to resolve distinct OA components from different sources. The PMF results were evaluated with an Igor Pro-based PMF Evaluation Tool (PET, v 2.04) (Ulbrich et al., 2009) following the procedures detailed in Zhang et al. (2011). After a careful evaluation of the spectral profiles, diurnal variations and correlations with external tracers, a 6-factor solution ($Q/Q_{exp} = 4.3$) was chosen, yielding a hydrocarbon-like OA (HOA), a cooking OA (COA), a coal combustion OA (CCOA), and three oxygenated OA (OOA) components. Because of the absence of collocated measurements to validate the different OOA components, the three OOA components were recombined into one OOA component. The contributions of four OA factors were relatively stable across different fpeak values (average ± 1σ; min – max, Fig. S4): HOA (14±1.6%; 12 – 16%), COA (14±2.8%; 11 – 17%), CCOA (19±2.7%; 15 – 22%), and OOA (51±1.7; 49 – 55%). However, considering the mass spectra of OA factors at fpeak = -1 presented the best correlation with those identified in winter 2011-2012 ($r^2 = 0.86 – 0.99$, Fig. S5) (Sun et al., 2013b), the four OA factors with fpeak = -1 was chosen in this study. The HOA spectrum resembles to that identified

by PMF analysis of high resolution OA mass spectra in Beijing in January 2013 (Zhang et al., 2014) which are both characterized pronounced *m/z* 91 and 115. Although the CCOA spectrum doesn't present similar pronounced *m/z*'s (e.g., 77, 91, 105, and 115) as that resolved at a rural site in Central Eastern China (Hu et al., 2013), it shows more similarity to that resolved in Beijing (Zhang et al., 2014). Also, CCOA correlates better with chloride with an importance source from coal combustion (Zhang et al., 2012) than HOA (r^2 = 0.41 vs. 0.24), and also correlates well with *m/z* 60 (r^2 = 0.77, Fig. S6) a tracer *m/z* for biomass burning (Cubison et al., 2011). Considering that the mass spectra and time series of HOA and CCOA are overall similar in this study, the PMF analysis may still have uncertainties in differentiation of the two factors. Particularly, ACSM does not measure high *m/z*'s (> 150) which are crucial (e.g., PAH signals) for distinguishing HOA and CCOA. Because we didn't have more external tracers to further validate these two factors, it is the best solution that we can get based on the current available data. Future work such as performing high-resolution time-of-flight AMS measurements or PMF analysis with the multi-linear engine (ME-2) algorithm (Paatero, 1999) are needed for a better investigation of HOA and CCOA in urban Beijing during wintertime. The sum of HOA and CCOA (= HOA+CCOA) correlates better with BC (r^2 = 0.88), NO_x (r^2 = 0.77), and CO (r^2 = 0.63) than HOA (r^2 = 0.36 – 0.47), which might suggest that coal combustion emissions are also important sources of CO, BC and NO_x during wintertime (Tian et al., 2008; Zhi et al., 2008). Although COA didn't have external tracers to validate, it is very distinct as suggested by its unique diurnal patterns (two peaks corresponding to meal time) and high *m/z* 55/57 ratio. Similar to our previous study (Sun et al., 2013b), the OOA shows a tight correlation with NO_3 (r^2 = 0.90) and also a good correlation with SO_4^{2-}+NO_3^- (r^2 = 0.87). The mass spectral profiles and

time series of four OA factors are shown in Fig. S6.

No biomass burning OA (BBOA) was resolved in this study. One of the reasons is that BBOA was likely not an important component of OA (e.g., < 5%), which is unlikely to be resolved accurately by PMF (Ulbrich et al., 2009). Indeed, we didn't observe strong biomass burning influences throughout the study by checking the scatter plot of f_{60} vs. f_{44} (Fig. S7). We found that f_{60} vs. f_{44} in Fig. S7 is outside of the typical biomass burning region (Cubison et al., 2011) for most of the time during this study. Although the average f_{60} (0.42%) is slightly higher than the typical value of f_{60} (~0.3%) in the absence of biomass burning impact (DeCarlo et al., 2008; Ulbrich et al., 2009), it is also likely due to the short range of *m/z* (12 – 120) used for the calculation of f_{60}. A summary of other key diagnostic plots of the PMF solution are given in Fig. S8 and Fig. S9.

3 Results and discussion

3.1 Identification and quantification of fireworks events

Burning of fireworks has been found to emit a large amount of K^+, which can be used to identify the FW events (Drewnick et al., 2006; Wang et al., 2007). As shown in Fig. 1 and Fig. 2, three FW events with significantly elevated K^+ were observed on the days of Lunar New Year (LNY, 9-10 February), Lunar Fifth Day (LFD, 14 February), and Lantern Festival (LF, 24 February), respectively. All three FW events started approximately at 18:00 and ended at midnight except LNY with a continuous FW impact until 4:00 on the second day (Fig. 2). Fig. 1 shows that the relative humidity was generally below 30% during LNY and LFD. While the wind speed at the ground surface remained consistently below 2 m s^{-1}, it was increased to ~ 4 m s^{-1} at the height of 100 m. Also note that there was a wind direction change in the middle

285 of the two events. The meteorological conditions during LF were stagnant with wind
286 speed generally below 2 m s^{-1} across different heights. The relative humidity was ~50%
287 and the temperature averaged 3.5°C.

288 To estimate the contributions of fireworks, we first assume that the background
289 concentration of each species has a linear variation during FW period. A linear fit was
290 then performed on the 6 h data before and after FW events. The difference between
291 the measured and the fitted value is assumed as the contribution from FW. The typical
292 examples for estimating FW contributions are shown in Fig. S10. It should be noted
293 that this approach might significantly overestimate the FW contributions of primary
294 species (e.g., HOA, COA, CCOA, and BC) that were largely enhanced during the
295 typical FW periods (18:00 – 24:00) due to the increased local emissions (see Fig. S11
296 for diurnal variations of aerosol species). However, it should have a minor impact on
297 secondary species (e.g., SO_4, NO_3, and OOA) because of their relatively stable
298 variations between 18:00-24:00. As shown in Fig.2, all aerosol species showed
299 substantial increases from 15:00 to 21:00 on the day of LNY which coincidently
300 corresponded to a gradual change of wind direction. Therefore, regional transport
301 might have played dominant roles for the evolution of chemical species during this
302 period. For these reasons, only the FW contributions between 23:30, 9 February and
303 3:30, 10 February when the meteorological conditions were stable were estimated.
304 The FW contributions during LFD might also be overestimated due to the influences
305 of regional transport as suggested by the wind direction change in the middle.

306 **3.2 Mass concentration and chemical composition of FW aerosols**

307 Figure 1 shows the time series of mass concentrations of PM_1, $PM_{2.5}$, and
308 submicron aerosol species from 1 February to 1 March 2013. Because ACSM cannot

309 measure the metals (e.g., Sr, Ba, Mg, etc.) that were significantly enhanced during
310 FW periods (Wang et al., 2007; Vecchi et al., 2008) , the PM_1 in this study refer to
311 NR-PM_1 (= Org + SO_4 + NO_3 + NH_4 + Chl+ K + KCl) + BC. The $PM_{2.5}$ showed three
312 prominent FW peaks with the maximum concentration occurring at ~00:30 during
313 LNY and ~21:30 during LFD and LF, respectively. The peak concentration of $PM_{2.5}$
314 during LNY (775 μg m^{-3}) is more than 10 times higher than the China National
315 Ambient Air Quality Standard (75 μg m^{-3}, 24 h average). The average FW-$PM_{2.5}$ mass
316 concentrations during three FW events all exceeded 100 μg m^{-3}. These results suggest
317 that fireworks have large impacts on fine particle pollution, yet generally less than
318 half day (approximately 10 h for LNY, and 6 h for LFD and LF). The PM_1 also
319 showed increases during the FW periods, yet not as significant as $PM_{2.5}$. In fact the
320 correlation of PM_1 versus $PM_{2.5}$ shows much lower $PM_1/PM_{2.5}$ (0.08 – 0.19) ratios
321 during three FW events than that observed during NFW periods (0.90) (Fig. 3). One
322 of the reasons is likely due to the mineral dust component and metals from fireworks
323 that ACSM did not measure. However, the ACSM un-detected metals (e.g., Mg, Sr,
324 and Ba) that are largely enhanced during FW periods generally contribute a small
325 fraction of PM (<2%) (Wang et al., 2007; Vecchi et al., 2008; Kong et al., 2015).
326 Therefore, our results might suggest that a large fraction of aerosol particles from the
327 burning of fireworks was emitted in the size range of 1 – 2.5 μm. It is also possible
328 that coagulations and VOCs condensation on the aerosol phase during FW period
329 played a role. Consistently, Vecchi et al. (2008) found the best correlation between
330 the fireworks tracer, Sr, and the particles between 700-800 nm (mobility diameter, D_m)
331 which is approximately equivalent to 1.9 – 2.2 μm in D_{va} (vacuum aerodynamic
332 diameter, D_{va}) with a density of 2.7 g cm^{-3} (Zhang et al., 2010).

Figure 4 shows the average chemical composition of PM_1 and OA from fireworks and also the background composition during LNY, LFD and LF. The background PM_1 during LNY and LFD showed typical characteristics of clean periods with high fraction of organics (> ~50%) (Sun et al., 2012; Sun et al., 2013b), whereas that during LF was dominated by SIA (52%). As a comparison, organics constituted the major fraction of FW-PM_1, contributing 44 – 55% on average. During LNY, FW exerted large impacts on potassium and chloride whose contributions were elevated to 21% and 15% of PM_1, respectively, from less than 7% (Chl) in the background aerosols. The large increases of potassium and chloride were also observed during LFD and LF, and previous studies in Beijing (Wang et al., 2007; Cheng et al., 2014). As shown in Fig. 4, FW also emitted a considerable amount of sulfate, accounting for 7% - 14% of PM_1. Sulfate correlated strongly with SO_2 during all three FW events (r^2 = 0.49 -0.92). Given that the relative humidity was low, < 30% during LNY and LFD, and ~ 50% during LF, aqueous-phase oxidation of SO_2 depending on liquid water content could not play significant roles for the sulfate formation (Sun et al., 2013a). Therefore, sulfate in FW-PM_1 was mainly from the direction emissions of FW. Compared to sulfate, FW appeared to show minor impacts on nitrate, for example, 4% and 2% during LNY and LF, respectively. Although nitrate contributed 12% of FW-PM_1 during LFD, most of it was likely from regional transport as supported by synchronous increases of all aerosol species associated with a wind direction change in the middle (Fig. 2).

The OOA contributed dominantly to OA during LNY, which is 79% on average (Fig. 4a). As shown in Fig. 5, the mass spectrum of FW-organics is highly similar to that of low-volatility OOA (LV-OOA, r^2 = 0.94; r^2 = 0.89 by excluding *m/z* 18 and

357 *m/z* 44) (Ng et al., 2011a) indicating that the FW-organics is likely emitted in
358 secondary. Consistently, Drewnick et al. (2006) also found large enhancements of the
359 OOA-related *m/z*'s (e.g., *m/z* 44) during New Year's fireworks, but the HOA-related
360 *m/z*'s (e.g., *m/z* 57) are not significant contributors to FW organics. OOA accounted
361 for a much smaller fraction of OA during LF (28%) due to the large contributions of
362 POA components (72%). Although the OOA contributions varied during three FW
363 events, their absolute concentrations were relatively close ranging from 5.8 to 7.9 μg
364 m^{-3}. It should be noted that our approach might overestimate the POA components in
365 FW-OA because of the influences of NFW sources, in particular during the FW
366 period of LF when the local HOA, COA, and CCOA happened to have large increases.
367 By excluding the POA components in FW-OA, FW on average contributed 15 – 19
368 μg m^{-3} PM_1 during three FW events.

369 **3.3 Secondary aerosol and PM pollution**

370 The PM_1 (NR-PM_1 + BC) varied largely across the entire study with daily average
371 mass concentration ranging from 9.1 to 169 μg m^{-3}. The average PM_1 mass
372 concentration was 80 (±68) μg m^{-3}, which is approximately 20% higher than that
373 observed during winter 2011-2012 (Sun et al., 2013b). Organics composed the major
374 fraction of PM_1 accounting for 43%, followed by nitrate (22%), sulfate (14%),
375 ammonium (13%), BC (5%) and chloride (3%). The OA composition was dominated
376 by OOA (53%) with the rest being POA. Compared to winter 2011-2012 (Sun et al.,
377 2013b), this study showed significantly enhanced OOA (53% vs. 31%) and secondary
378 nitrate (22% vs. 16%), indicating that secondary formation have played important
379 roles in the formation of pollution episodes.

380 Figure 1d shows that submicron aerosol species alternated routinely between

pollution events (PEs) and clean periods (CPs) throughout the entire study. The PEs generally lasted ~1 – 2 days except the one on 23 – 28 February that lasted more than 5 days, whereas the CPs were shorter, generally less than 1 day. In total, 9 PEs and 9 CPs were identified in this study (Fig. 1). A statistics of the mass concentrations and mass fractions of aerosol species during 9 PEs is presented in Fig. 6. The average PM_1 mass concentration ranged 68 – 179 μg m^{-3} during PEs with the total secondary particulate matter (SPM = OOA + SO_4 + NO_3 +NH_4) accounting for 63 – 82%. The average mass concentration of SPM for the 9 PEs was 86 (±32) μg m^{-3}, which is nearly 3 times that of primary PM (PPM = HOA + COA +CCOA + BC + Chl) (30 ±9.5 μg m^{-3}). SPM consistently dominated PM_1 across different PM levels (69 – 75%), but generally with higher contributions (up to 81%) during daytime (Fig. 7b). The diurnal cycle of SPM presented a gradual increase from 50 to 70 μg m^{-3} between 10:00 – 20:00, indicating evident photochemical production of secondary species during daytime. It should be also noted that all secondary species showed ubiquitously higher mass concentrations than those of primary species (Fig. 6a).

The SOA generally contributed more than 50% to OA with an average of 55% during PEs except the episode on 3 February (35%). It's interesting to note that the contribution of POA increased as a function of organic loadings which varied from ~35% to 63% when organics was above 80 μg m^{-3} (Fig. 7c). Such behavior is mainly caused by the enhanced CCOA at high organic mass loadings, which was also observed during winter 2011 – 2012 (Sun et al., 2013b). These results suggest that POA played more important roles than SOA in PM pollution during periods with high organic mass loadings (e.g., > 60 μg m^{-3}). In fact, POA showed even higher mass concentration than OOA at nighttime (0:00 – 8:00) due to the intensified local

emissions, e.g., coal combustion for heating. Despite this, the role of POA in PM pollution was compensated by the elevated secondary inorganic species as a function of PM loadings (Fig. 7a) leading to the consistently dominant SPM across different pollution levels. Figure 8a shows an evidently lower contribution of organics to PM_1 during PEs than CPs. The elevated secondary inorganic species during PEs were closely related to the increase of RH (Fig. 1). For example, during the pollution episode on 3 February, the sulfate concentration increased rapidly and became the major inorganic species when RH was increased from ~60% to > 90%. The gaseous SO_2 showed a corresponding decrease indicating aqueous-phase processing of SO_2 to form sulfate, consistent with our previous conclusion that aqueous-phase processing could contribute more than 50% of sulfate production during winter 2011-2012 (Sun et al., 2013a).

The compositional differences between PEs and CPs also led to different mass extinction efficiency (MEE, 630 nm) of PM_1 (Fig. 8b). The higher MEE (6.4 m^2 g^{-1}) during PEs than CPs (4.4 m^2 g^{-1}) is primarily due to the enhanced secondary species, and also likely the increases of aerosol particle sizes although we don't have size data to support it. Similar increases of mass scattering efficiency from clean periods to relatively polluted conditions were also observed previously in Beijing and Shanghai (Jung et al., 2009; Huang et al., 2013). It should be noted that the MEE of PM_1 in this study refers to $PM_{2.5}$ b_{ext}/PM_1. Considering that PM_1 on average contributes ~60-70% of $PM_{2.5}$ in Beijing (Sun et al., 2012; Sun et al., 2013b), the real MEE of PM_1 during PEs and CPs would be ~3.8 - 4.5 and ~2.6 - 3.1 m^2 g^{-1}, respectively.

3.4 Holiday effects on PM pollution

Figure 9 shows a comparison of aerosol species, gaseous species, and

meteorological parameters between holiday (HD) and non-holiday (NHD) periods. The official holiday for the Spring Festival was 9 – 15 February. However, we noted a large decrease of cooking aerosols from 7 February until 19 February (Fig. S6b), whose emissions were expected to be stable under similar meteorological conditions. The decrease of COA was likely due to the reduction of the number of population in Beijing, which agreed with the fact that most migrants from outside Beijing were leaving for hometown before the official holiday. Therefore, 7 – 19 February was used as a longer holiday for a comparison. It was estimated that approximately half of population (9 million) left Beijing before the Spring Festival (http://news.xinhuanet.com/yzyd/local/20130208/c_114658765.htm). Such a great reduction in human activities would exert a large impact on aerosol composition and sources in the city during holidays. To better investigate the HD effects on PM pollution, the data shown in Fig. 9 excluded the CPs marked in Fig. 1. The data with the CPs included are presented in Fig. S12.

The differences between HD and NHD for primary species varied largely among different species. COA showed the largest reduction (69%) among aerosol species with the average concentration decreasing from 5.8 μg m^{-3} during NHD to 1.8 μg m^{-3} during HD. The contribution of COA to OA showed a corresponding decrease from 12% to 4%. Given the similar meteorological conditions between HD and NHD, e.g., RH (46% vs. 52%) and wind speed (1.3 m s^{-1} vs. 1.2 m s^{-1}), the reduction of COA clearly indicated a large decrease of population and the number of restaurants opened during HD. The CCOA showed approximately 30% reduction during HD, and its contribution to OA decreased from 23% to 18%. Not surprisingly, chloride showed a similar reduction as CCOA because it was primarily from coal combustion emissions

453 during wintertime (Sun et al., 2013b). Figure 9 also shows a significant reduction
454 (54%) for NO indicating much less traffic emissions in the city during HD. The HOA,
455 however, even showed a slight increase during HD, which appeared to contradict with
456 the reduction of two combustion-related tracers, BC and CO (~20%). This can be
457 explained by the fact that coal combustion is a large source of BC and CO during
458 heating season (Tian et al., 2008; Zhi et al., 2008). Consistently, BC and CO showed
459 relatively similar reductions to CCOA. Therefore, the minor variation of HOA might
460 indicate that the number of heavy-duty vehicles and diesel trucks that dominated
461 HOA emissions (Massoli et al., 2012; Hayes et al., 2013) remained little change
462 during HD period although that of gasoline vehicles was largely decreased. It should
463 be noted that HOA showed a large peak on 9 February – the first day of the official
464 holiday (Fig. S6b) when more traffic emissions were expected due to many people
465 leaving for hometown. After that, HOA showed slightly lower concentration during
466 11 – 17 February than other periods. In fact, the average HOA showed a slight
467 reduction (~5%) during the long holiday period (7 – 19 February) suggesting a small
468 holiday effect on HOA reduction. Together, the total primary aerosol species (PPM)
469 showed an average reduction of 22% because of holiday effects.

470 Nitrate showed the largest reduction among secondary species by 22% during HD,
471 primarily due to a reduction of its precursors NO and NO_2. The results suggest that
472 reducing traffic emissions would help mitigate the nitrate pollution in the city.
473 Compared to nitrate, sulfate showed minor changes (2%) between HD and NHD, and
474 OOA even showed a slight increase (6%) during HD. One of the reasons is that
475 secondary sulfate and OOA were mainly formed over regional scale and less affected
476 by local production, consistent with their relatively flat diurnal cycles (Fig. S11).

Ammonium showed a reduction between nitrate and sulfate because ammonium mainly existed in the form of $(NH_4)_2SO_4$ and NH_4NO_3. Overall, secondary species showed generally lower reductions than primary species with the total secondary species (SPM) showing an average reduction of 9% during HD. The joint reductions of PPM and SPM led to an average reduction of 13% for PM_1 during HD. However, these reductions did not help alleviate the fine particle pollution during HD. The $PM_{2.5}$ excluding FW impacts even showed 27% increase from 96 μg m^{-3} during NHD to 122 μg m^{-3} during HD. One possible reason is likely due to the increases of aerosol species in the size range of 1 – 2.5 μm during HD period. The longer holiday (LHD, 7 – 19 February) showed similar influences on both primary and secondary species as the official holiday (9 – 15 February). COA, CCOA, and NO are the three species with the largest reductions during LHD (> 50%). However, HOA, SO_4, OOA, and $PM_{2.5}$ showed rather small changes (< ±7%). Therefore, results in this study suggest that controlling the primary source emissions, e.g., cooking and traffic emissions in the city can reduce the primary particles largely, yet has limited effects on secondary species and the total fine particle mass. One of the reasons is because the severe PM pollution in Beijing is predominantly contributed by secondary species (see discussions in section 3.3) that are formed over regional scales. Reducing the primary source emissions in local areas would have limited impacts on mitigation of air pollution in the city. Similarly, Guo et al. (2013) reported a large reduction of primary organic carbon (OC) from traffic emissions and coal combustion during the 2008 Olympic Summer Games when traffic restrictions and temporary closure of factories were implemented. However, secondary OC was not statistically different between controlled and non-controlled periods. Our results highlight the importance of

501 implementing joint efforts over regional scales for air pollution control in north
502 China.

503 **4 Conclusions**

504 We have characterized the aerosol particle composition and sources during the
505 Chinese Spring Festival in 2013. The average PM_1 mass concentration was 80 (±68)
506 μg m^{-3} for the entire study with organics being the major fraction (43%). Nine
507 pollution events and nine clean periods with substantial compositional differences
508 were observed. The secondary particulate matter (= SOA+ sulfate + nitrate +
509 ammonium) played a dominant role for the PM pollution during nine PEs. The
510 contributions of SPM to PM_1 varied from 63% to 82% with SOA on average
511 accounting for ~55% of OA. As a result, the average mass extinction efficiency of
512 PM_1 during PEs (6.4 m^2 g^{-1}) was higher than that during CPs (4.4 m^2 g^{-1}). Three FW
513 events, i.e., LNY, LFD, and LF, were identified, which showed significant and
514 short-term impacts on fine particles, and non-refractory potassium, chloride, and
515 sulfate in PM_1. The FW also exerted a large impact on organics that presented mainly
516 in secondary as indicated by its similar mass spectrum to that of oxygenated OA. The
517 holiday effects on aerosol composition and sources were also investigated by
518 comparing the differences between holiday and non-holiday periods. The changes of
519 anthropogenic source emissions during the holiday showed large impacts on reduction
520 of cooking OA (69%), nitrogen monoxide (54%), and coal combustion OA (28%) in
521 the city, yet presented much smaller influences on secondary species. The average
522 SOA and the total $PM_{2.5}$ even increased slightly during the holiday period. Results
523 here have significant implications that controlling the local primary source emissions,
524 e.g., cooking and traffic activities, might have limited effects on improving air quality

during polluted days when SPM from regional transport dominated aerosol composition for most of time. Our results also highlight the importance of implementing joint measures over regional scales for mitigation of air pollution in megacity Beijing.

Acknowledgements

This work was supported by the National Key Project of Basic Research (2014CB447900), the Strategic Priority Research Program (B) of the Chinese Academy of Sciences (Grant No. XDB05020501), and the National Natural Science Foundation of China (41175108). We thank Huabin Dong, Hongyan Chen, and Zhe Wang's help in data collection, and also the Technical and Service Center, Institute of Atmospheric Physics, Chinese Academy of Sciences for providing meteorological data.

References

Budisulistiorini, S. H., Canagaratna, M. R., Croteau, P. L., Baumann, K., Edgerton, E. S., Kollman, M. S., Ng, N. L., Verma, V., Shaw, S. L., Knipping, E. M., Worsnop, D. R., Jayne, J. T., Weber, R. J., and Surratt, J. D.: Intercomparison of an Aerosol Chemical Speciation Monitor (ACSM) with ambient fine aerosol measurements in downtown Atlanta, Georgia, Atmos. Meas. Tech., 7, 1929-1941, 10.5194/amt-7-1929-2014, 2014.

Chan, C. K., and Yao, X.: Air pollution in mega cities in China, Atmos. Environ., 42, 1-42, DOI: 10.1016/j.atmosenv.2007.09.003, 2008.

Cheng, Y., Engling, G., He, K.-B., Duan, F.-K., Du, Z.-Y., Ma, Y.-L., Liang, L.-L., Lu, Z.-F., Liu, J.-M., Zheng, M., and Weber, R. J.: The characteristics of Beijing aerosol during two distinct episodes: Impacts of biomass burning and fireworks, Environ. Pollut., 185, 149-157, http://dx.doi.org/10.1016/j.envpol.2013.10.037, 2014.

Cubison, M. J., Ortega, A. M., Hayes, P. L., Farmer, D. K., Day, D., Lechner, M. J., Brune, W. H., Apel, E., Diskin, G. S., Fisher, J. A., Fuelberg, H. E., Hecobian, A.,

555 Knapp, D. J., Mikoviny, T., Riemer, D., Sachse, G. W., Sessions, W., Weber, R. J.,
556 Weinheimer, A. J., Wisthaler, A., and Jimenez, J. L.: Effects of aging on organic
557 aerosol from open biomass burning smoke in aircraft and laboratory studies,
558 Atmos. Chem. Phys., 11, 12049-12064, 10.5194/acp-11-12049-2011, 2011.
559 DeCarlo, P. F., Kimmel, J. R., Trimborn, A., Northway, M. J., Jayne, J. T., Aiken, A.
560 C., Gonin, M., Fuhrer, K., Horvath, T., Docherty, K. S., Worsnop, D. R., and
561 Jimenez, J. L.: Field-Deployable, High-Resolution, Time-of-Flight Aerosol Mass
562 Spectrometer, Anal. Chem., 78, 8281-8289, 2006.
563 DeCarlo, P. F., Dunlea, E. J., Kimmel, J. R., Aiken, A. C., Sueper, D., Crounse, J.,
564 Wennberg, P. O., Emmons, L., Shinozuka, Y., Clarke, A., Zhou, J., Tomlinson, J.,
565 Collins, D. R., Knapp, D., Weinheimer, A. J., Montzka, D. D., Campos, T., and
566 Jimenez, J. L.: Fast airborne aerosol size and chemistry measurements above
567 Mexico City and Central Mexico during the MILAGRO campaign, Atmos. Chem.
568 Phys., 8, 4027-4048, 2008.
569 DeCarlo, P. F., Ulbrich, I. M., Crounse, J., de Foy, B., Dunlea, E. J., Aiken, A. C.,
570 Knapp, D., Weinheimer, A. J., Campos, T., Wennberg, P. O., and Jimenez, J. L.:
571 Investigation of the sources and processing of organic aerosol over the Central
572 Mexican Plateau from aircraft measurements during MILAGRO, Atmos. Chem.
573 Phys., 10, 5257-5280, 10.5194/acp-10-5257-2010, 2010.
574 Drewnick, F., Hings, S. S., Curtius, J., Eerdekens, G., and Williams, J.: Measurement
575 of fine particulate and gas-phase species during the New Year's fireworks 2005 in
576 Mainz, Germany, Atmos. Environ., 40, 4316-4327,
577 10.1016/j.atmosenv.2006.03.040, 2006.
578 Duan, F. K., He, K. B., Ma, Y. L., Yang, F. M., Yu, X. C., Cadle, S. H., Chan, T., and
579 Mulawa, P. A.: Concentration and chemical characteristics of PM2.5 in Beijing,
580 China: 2001–2002, Sci. Total Environ., 355, 264-275,
581 10.1016/j.scitotenv.2005.03.001, 2006.
582 Feng, J., Sun, P., Hu, X., Zhao, W., Wu, M., and Fu, J.: The chemical composition
583 and sources of PM2.5 during the 2009 Chinese New Year's holiday in Shanghai,
584 Atmospheric Research, 118, 435-444,
585 http://dx.doi.org/10.1016/j.atmosres.2012.08.012, 2012.
586 Godri, K. J., Green, D. C., Fuller, G. W., Dall'Osto, M., Beddows, D. C., Kelly, F. J.,
587 Harrison, R. M., and Mudway, I. S.: Particulate oxidative burden associated with
588 firework activity, Environ. Sci. Technol., 44, 8295-8301, 2010.
589 Guo, S., Hu, M., Wang, Z. B., Slanina, J., and Zhao, Y. L.: Size-resolved aerosol
590 water-soluble ionic compositions in the summer of Beijing: implication of
591 regional secondary formation, Atmos. Chem. Phys., 10, 947-959,
592 10.5194/acp-10-947-2010, 2010.
593 Guo, S., Hu, M., Guo, Q., Zhang, X., Schauer, J. J., and Zhang, R.: Quantitative
594 evaluation of emission controls on primary and secondary organic aerosol sources
595 during Beijing 2008 Olympics, Atmos. Chem. Phys., 13, 8303-8314,
596 10.5194/acp-13-8303-2013, 2013.

Hayes, P. L., Ortega, A. M., Cubison, M. J., Froyd, K. D., Zhao, Y., Cliff, S. S., Hu, W. W., Toohey, D. W., Flynn, J. H., Lefer, B. L., Grossberg, N., Alvarez, S., Rappenglück, B., Taylor, J. W., Allan, J. D., Holloway, J. S., Gilman, J. B., Kuster, W. C., de Gouw, J. A., Massoli, P., Zhang, X., Liu, J., Weber, R. J., Corrigan, A. L., Russell, L. M., Isaacman, G., Worton, D. R., Kreisberg, N. M., Goldstein, A. H., Thalman, R., Waxman, E. M., Volkamer, R., Lin, Y. H., Surratt, J. D., Kleindienst, T. E., Offenberg, J. H., Dusanter, S., Griffith, S., Stevens, P. S., Brioude, J., Angevine, W. M., and Jimenez, J. L.: Organic aerosol composition and sources in Pasadena, California during the 2010 CalNex campaign, Journal of Geophysical Research: Atmospheres, 118, 9233–9257, 10.1002/jgrd.50530, 2013.

He, L.-Y., Huang, X.-F., Xue, L., Hu, M., Lin, Y., Zheng, J., Zhang, R., and Zhang, Y.-H.: Submicron aerosol analysis and organic source apportionment in an urban atmosphere in Pearl River Delta of China using high-resolution aerosol mass spectrometry, J. Geophys. Res., 116, D12304, 10.1029/2010jd014566, 2011.

Hu, W. W., Hu, M., Yuan, B., Jimenez, J. L., Tang, Q., Peng, J. F., Hu, W., Shao, M., Wang, M., Zeng, L. M., Wu, Y. S., Gong, Z. H., Huang, X. F., and He, L. Y.: Insights on organic aerosol aging and the influence of coal combustion at a regional receptor site of central eastern China, Atmos. Chem. Phys., 13, 10095-10112, 10.5194/acp-13-10095-2013, 2013.

Huang, K., Zhuang, G., Lin, Y., Wang, Q., Fu, J. S., Zhang, R., Li, J., Deng, C., and Fu, Q.: Impact of anthropogenic emission on air quality over a megacity – revealed from an intensive atmospheric campaign during the Chinese Spring Festival, Atmos. Chem. Phys., 12, 11631-11645, 10.5194/acp-12-11631-2012, 2012.

Huang, R.-J., Zhang, Y., Bozzetti, C., Ho, K.-F., Cao, J.-J., Han, Y., Daellenbach, K. R., Slowik, J. G., Platt, S. M., Canonaco, F., Zotter, P., Wolf, R., Pieber, S. M., Bruns, E. A., Crippa, M., Ciarelli, G., Piazzalunga, A., Schwikowski, M., Abbaszade, G., Schnelle-Kreis, J., Zimmermann, R., An, Z., Szidat, S., Baltensperger, U., Haddad, I. E., and Prevot, A. S. H.: High secondary aerosol contribution to particulate pollution during haze events in China, Nature, 514, 218 - 222, 10.1038/nature13774, 2014.

Huang, X. F., He, L. Y., Hu, M., Canagaratna, M. R., Sun, Y., Zhang, Q., Zhu, T., Xue, L., Zeng, L. W., Liu, X. G., Zhang, Y. H., Jayne, J. T., Ng, N. L., and Worsnop, D. R.: Highly time-resolved chemical characterization of atmospheric submicron particles during 2008 Beijing Olympic Games using an Aerodyne High-Resolution Aerosol Mass Spectrometer, Atmos. Chem. Phys., 10, 8933-8945, 10.5194/acp-10-8933-2010, 2010.

Huang, Y., Li, L., Li, J., Wang, X., Chen, H., Chen, J., Yang, X., Gross, D. S., Wang, H., Qiao, L., and Chen, C.: A case study of the highly time-resolved evolution of aerosol chemical and optical properties in urban Shanghai, China, Atmos. Chem. Phys., 13, 3931-3944, 10.5194/acp-13-3931-2013, 2013.

638 Jayne, J. T., Leard, D. C., Zhang, X., Davidovits, P., Smith, K. A., Kolb, C. E., and
639 Worsnop, D. R.: Development of an aerosol mass spectrometer for size and
640 composition analysis of submicron particles, Aerosol Sci. Tech., 33, 49-70, 2000.
641 Jung, J., Lee, H., Kim, Y. J., Liu, X., Zhang, Y., Hu, M., and Sugimoto, N.: Optical
642 properties of atmospheric aerosols obtained by in situ and remote measurements
643 during 2006 Campaign of Air Quality Research in Beijing (CAREBeijing-2006), J.
644 Geophys. Res., 114, D00G02, 10.1029/2008jd010337, 2009.
645 Kong, S. F., Li, L., Li, X. X., Yin, Y., Chen, K., Liu, D. T., Yuan, L., Zhang, Y. J.,
646 Shan, Y. P., and Ji, Y. Q.: The impacts of firework burning at the Chinese Spring
647 Festival on air quality: insights of tracers, source evolution and aging processes,
648 Atmos. Chem. Phys., 15, 2167-2184, 10.5194/acp-15-2167-2015, 2015.
649 Li, W., Shi, Z., Yan, C., Yang, L., Dong, C., and Wang, W.: Individual metal-bearing
650 particles in a regional haze caused by firecracker and firework emissions, Sci.
651 Total Environ., 443, 464-469, http://dx.doi.org/10.1016/j.scitotenv.2012.10.109,
652 2013.
653 Liu, X. G., Li, J., Qu, Y., Han, T., Hou, L., Gu, J., Chen, C., Yang, Y., Liu, X., Yang,
654 T., Zhang, Y., Tian, H., and Hu, M.: Formation and evolution mechanism of
655 regional haze: a case study in the megacity Beijing, China, Atmos. Chem. Phys.,
656 13, 4501-4514, 10.5194/acp-13-4501-2013, 2013.
657 Massoli, P., Kebabian, P. L., Onasch, T. B., Hills, F. B., and Freedman, A.: Aerosol
658 light extinction measurements by Cavity Attenuated Phase Shift (CAPS)
659 spectroscopy: Laboratory validation and field deployment of a compact aerosol
660 particle extinction monitor, Aerosol Sci. Tech., 44, 428-435,
661 10.1080/02786821003716599, 2010.
662 Massoli, P., Fortner, E. C., Canagaratna, M. R., Williams, L. R., Zhang, Q., Sun, Y.,
663 Schwab, J. J., Trimborn, A., Onasch, T. B., Demerjian, K. L., Kolb, C. E.,
664 Worsnop, D. R., and Jayne, J. T.: Pollution gradients and chemical
665 characterization of particulate matter from vehicular traffic near major roadways:
666 Results from the 2009 Queens College Air Quality Study in NYC, Aerosol Sci.
667 Tech., 46, 1201-1218, 10.1080/02786826.2012.701784, 2012.
668 Matsui, H., Koike, M., Kondo, Y., Takegawa, N., Kita, K., Miyazaki, Y., Hu, M.,
669 Chang, S. Y., Blake, D. R., Fast, J. D., Zaveri, R. A., Streets, D. G., Zhang, Q.,
670 and Zhu, T.: Spatial and temporal variations of aerosols around Beijing in summer
671 2006: Model evaluation and source apportionment, J. Geophys. Res., 114,
672 D00G13, 10.1029/2008jd010906, 2009.
673 Matthew, B. M., Middlebrook, A. M., and Onasch, T. B.: Collection Efficiencies in an
674 Aerodyne Aerosol Mass Spectrometer as a Function of Particle Phase for
675 Laboratory Generated Aerosols, Aerosol Sci. Tech., 42, 884 - 898, 2008.
676 Middlebrook, A. M., Bahreini, R., Jimenez, J. L., and Canagaratna, M. R.: Evaluation
677 of composition-dependent collection efficiencies for the Aerodyne Aerosol Mass
678 Spectrometer using field data, Aerosol Sci. Tech., 46, 258-271, 2012.
679 Molina, M. J., and Molina, L. T.: Megacities and atmospheric pollution, J. Air Waste
680 Manage. Assoc., 54, 644–680, 2004.

Moreno, T., Querol, X., Alastuey, A., Cruz Minguillón, M., Pey, J., Rodriguez, S., Vicente Miró, J., Felis, C., and Gibbons, W.: Recreational atmospheric pollution episodes: Inhalable metalliferous particles from firework displays, Atmos. Environ., 41, 913-922, http://dx.doi.org/10.1016/j.atmosenv.2006.09.019, 2007.

Ng, N. L., Canagaratna, M. R., Jimenez, J. L., Zhang, Q., Ulbrich, I. M., and Worsnop, D. R.: Real-time methods for estimating organic component mass concentrations from Aerosol Mass Spectrometer data, Environ. Sci. Technol., 45, 910-916, 10.1021/es102951k, 2011a.

Ng, N. L., Herndon, S. C., Trimborn, A., Canagaratna, M. R., Croteau, P. L., Onasch, T. B., Sueper, D., Worsnop, D. R., Zhang, Q., Sun, Y. L., and Jayne, J. T.: An Aerosol Chemical Speciation Monitor (ACSM) for routine monitoring of the composition and mass concentrations of ambient aerosol, Aerosol Sci. Tech., 45, 770 - 784, 2011b.

Paatero, P., and Tapper, U.: Positive matrix factorization: A non-negative factor model with optimal utilization of error estimates of data values, Environmetrics, 5, 111-126, 1994.

Paatero, P.: The multilinear engine - A table-driven, least squares program for solving multilinear problems, including the n-way parallel factor analysis model, Journal of Computational and Graphical Statistics, 8, 854-888, 1999.

Petit, J. E., Favez, O., Sciare, J., Canonaco, F., Croteau, P., Močnik, G., Jayne, J., Worsnop, D., and Leoz-Garziandia, E.: Submicron aerosol source apportionment of wintertime pollution in Paris, France by double positive matrix factorization (PMF2) using an aerosol chemical speciation monitor (ACSM) and a multi-wavelength Aethalometer, Atmos. Chem. Phys., 14, 13773-13787, 10.5194/acp-14-13773-2014, 2014.

Slowik, J. G., Stroud, C., Bottenheim, J. W., Brickell, P. C., Chang, R. Y. W., Liggio, J., Makar, P. A., Martin, R. V., Moran, M. D., Shantz, N. C., Sjostedt, S. J., van Donkelaar, A., Vlasenko, A., Wiebe, H. A., Xia, A. G., Zhang, J., Leaitch, W. R., and Abbatt, J. P. D.: Characterization of a large biogenic secondary organic aerosol event from eastern Canadian forests, Atmos. Chem. Phys., 10, 2825-2845, 2010.

Song, Y., Zhang, Y., Xie, S., Zeng, L., Zheng, M., Salmon, L. G., Shao, M., and Slanina, S.: Source apportionment of $PM_{2.5}$ in Beijing by positive matrix factorization, Atmos. Environ., 40, 1526-1537, DOI: 10.1016/j.atmosenv.2005.10.039, 2006.

Sun, J., Zhang, Q., Canagaratna, M. R., Zhang, Y., Ng, N. L., Sun, Y., Jayne, J. T., Zhang, X., Zhang, X., and Worsnop, D. R.: Highly time- and size-resolved characterization of submicron aerosol particles in Beijing using an Aerodyne Aerosol Mass Spectrometer, Atmos. Environ., 44, 131-140, 2010.

Sun, Y., Zhuang, G., Tang, A., Wang, Y., and An, Z.: Chemical Characteristics of $PM_{2.5}$ and PM_{10} in Haze-Fog Episodes in Beijing, Environ. Sci. Technol., 40, 3148-3155, 2006.

723 Sun, Y. L., Wang, Z., Dong, H., Yang, T., Li, J., Pan, X., Chen, P., and Jayne, J. T.:
724 Characterization of summer organic and inorganic aerosols in Beijing, China with
725 an Aerosol Chemical Speciation Monitor, Atmos. Environ., 51, 250-259,
726 10.1016/j.atmosenv.2012.01.013, 2012.
727 Sun, Y. L., Wang, Z., Fu, P., Jiang, Q., Yang, T., Li, J., and Ge, X.: The impact of
728 relative humidity on aerosol composition and evolution processes during
729 wintertime in Beijing, China, Atmos. Environ., 77, 927–934,
730 http://dx.doi.org/10.1016/j.atmosenv.2013.06.019, 2013a.
731 Sun, Y. L., Wang, Z. F., Fu, P. Q., Yang, T., Jiang, Q., Dong, H. B., Li, J., and Jia, J.
732 J.: Aerosol composition, sources and processes during wintertime in Beijing,
733 China, Atmos. Chem. Phys., 13, 4577-4592, 10.5194/acp-13-4577-2013, 2013b.
734 Sun, Y. L., Jiang, Q., Wang, Z., Fu, P., Li, J., Yang, T., and Yin, Y.: Investigation of
735 the sources and evolution processes of severe haze pollution in Beijing in January
736 2013, J. Geophys. Res., 119, 4380-4398, 10.1002/2014JD021641, 2014.
737 Tian, L., Lucas, D., Fischer, S. L., Lee, S. C., Hammond, S. K., and Koshland, C. P.:
738 Particle and Gas Emissions from a Simulated Coal-Burning Household Fire Pit,
739 Environ. Sci. Technol., 42, 2503-2508, 10.1021/es0716610, 2008.
740 Tian, Y. Z., Wang, J., Peng, X., Shi, G. L., and Feng, Y. C.: Estimation of the direct
741 and indirect impacts of fireworks on the physicochemical characteristics of
742 atmospheric PM10 and PM2.5, Atmos. Chem. Phys., 14, 9469-9479,
743 10.5194/acp-14-9469-2014, 2014.
744 Ulbrich, I. M., Canagaratna, M. R., Zhang, Q., Worsnop, D. R., and Jimenez, J. L.:
745 Interpretation of organic components from Positive Matrix Factorization of
746 aerosol mass spectrometric data, Atmos. Chem. Phys., 9, 2891-2918, 2009.
747 Vecchi, R., Bernardoni, V., Cricchio, D., D'Alessandro, A., Fermo, P., Lucarelli, F.,
748 Nava, S., Piazzalunga, A., and Valli, G.: The impact of fireworks on airborne
749 particles, Atmos. Environ., 42, 1121-1132, 10.1016/j.atmosenv.2007.10.047,
750 2008.
751 Wang, Y., Zhuang, G., Sun, Y., and An, Z.: The variation of characteristics and
752 formation mechanisms of aerosols in dust, haze, and clear days in Beijing, Atmos.
753 Environ., 40, 6579-6591, 2006.
754 Wang, Y., Zhuang, G., Xu, C., and An, Z.: The air pollution caused by the burning of
755 fireworks during the lantern festival in Beijing, Atmos. Environ., 41, 417-431,
756 10.1016/j.atmosenv.2006.07.043, 2007.
757 Wang, Y., Yao, L., Wang, L., Liu, Z., Ji, D., Tang, G., Zhang, J., Sun, Y., Hu, B., and
758 Xin, J.: Mechanism for the formation of the January 2013 heavy haze pollution
759 episode over central and eastern China, Sci. China Earth Sci., 57, 14-25,
760 10.1007/s11430-013-4773-4, 2014.
761 Yang, F., Tan, J., Zhao, Q., Du, Z., He, K., Ma, Y., Duan, F., and Chen, G.:
762 Characteristics of $PM_{2.5}$ speciation in representative megacities and across China,
763 Atmos. Chem. Phys., 11, 5207-5219, 10.5194/acp-11-5207-2011, 2011.
764 Yang, L., Gao, X., Wang, X., Nie, W., Wang, J., Gao, R., Xu, P., Shou, Y., Zhang, Q.,
765 and Wang, W.: Impacts of firecracker burning on aerosol chemical characteristics

766 and human health risk levels during the Chinese New Year Celebration in Jinan,
767 China, Sci. Total Environ., 476–477, 57-64,
768 http://dx.doi.org/10.1016/j.scitotenv.2013.12.110, 2014.
769 Yao, X., Chan, C. K., Fang, M., Cadle, S., Chan, T., Mulawa, P., He, K., and Ye, B.:
770 The water-soluble ionic composition of PM2.5 in Shanghai and Beijing, China,
771 Atmos. Environ., 36, 4223-4234, Doi: 10.1016/s1352-2310(02)00342-4, 2002.
772 Zhang, H., Wang, S., Hao, J., Wan, L., Jiang, J., Zhang, M., Mestl, H. E. S., Alnes, L.
773 W. H., Aunan, K., and Mellouki, A. W.: Chemical and size characterization of
774 particles emitted from the burning of coal and wood in rural households in
775 Guizhou, China, Atmos. Environ., 51, 94-99, 10.1016/j.atmosenv.2012.01.042,
776 2012.
777 Zhang, J. K., Sun, Y., Liu, Z. R., Ji, D. S., Hu, B., Liu, Q., and Wang, Y. S.:
778 Characterization of submicron aerosols during a month of serious pollution in
779 Beijing, 2013, Atmos. Chem. Phys., 14, 2887-2903, 10.5194/acp-14-2887-2014,
780 2014.
781 Zhang, M., Wang, X., Chen, J., Cheng, T., Wang, T., Yang, X., Gong, Y., Geng, F.,
782 and Chen, C.: Physical characterization of aerosol particles during the Chinese
783 New Year's firework events, Atmos. Environ., 44, 5191-5198,
784 10.1016/j.atmosenv.2010.08.048, 2010.
785 Zhang, Q., Jimenez, J., Canagaratna, M., Ulbrich, I., Ng, N., Worsnop, D., and Sun,
786 Y.: Understanding atmospheric organic aerosols via factor analysis of aerosol
787 mass spectrometry: a review, Anal. Bioanal. Chem., 401, 3045-3067,
788 10.1007/s00216-011-5355-y, 2011.
789 Zhang, R., Jing, J., Tao, J., Hsu, S. C., Wang, G., Cao, J., Lee, C. S. L., Zhu, L., Chen,
790 Z., Zhao, Y., and Shen, Z.: Chemical characterization and source apportionment
791 of $PM_{2.5}$ in Beijing: seasonal perspective, Atmos. Chem. Phys., 13, 7053-7074,
792 10.5194/acp-13-7053-2013, 2013.
793 Zhao, S., Yu, Y., Yin, D., Liu, N., and He, J.: Ambient particulate pollution during
794 Chinese Spring Festival in urban Lanzhou, Northwestern China, Atmospheric
795 Pollution Research, 5, 335-343, doi: 10.5094/APR.2014.039, 2014.
796 Zhao, X. J., Zhao, P. S., Xu, J., Meng, W., Pu, W. W., Dong, F., He, D., and Shi, Q.
797 F.: Analysis of a winter regional haze event and its formation mechanism in the
798 North China Plain, Atmos. Chem. Phys., 13, 5685-5696,
799 10.5194/acp-13-5685-2013, 2013.
800 Zheng, M., Salmon, L. G., Schauer, J. J., Zeng, L., Kiang, C. S., Zhang, Y., and Cass,
801 G. R.: Seasonal trends in $PM_{2.5}$ source contributions in Beijing, China, Atmos.
802 Environ., 39, 3967-3976, DOI: 10.1016/j.atmosenv.2005.03.036, 2005.
803 Zhi, G., Chen, Y., Feng, Y., Xiong, S., Li, J., Zhang, G., Sheng, G., and Fu, J.:
804 Emission characteristics of carbonaceous particles from various residential
805 coal-stoves in China, Environ. Sci. Technol., 42, 3310-3315, 2008.

Figure captions:

Figure 1. Time series of meteorological parameters (a) relative humidity (RH) and temperature (T); (b) wind direction (WD) and wind speed (WS) at the height of 8m and 100 m; mass concentrations of (c) $PM_{2.5}$ and NR-PM_1 + BC and (d) submicron aerosol species. The extinction coefficient (b_{ext}) at 630 nm is shown in (c). Three events, i.e., Lunar New Year (LNY), Lunar Fifth Day (LFD) and Lantern Festival (LF) with significant influences of fireworks are marked in (c). In addition, the classified clean periods (CPs) and polluted events (PEs) are marked as shaded light blue and pink areas, respectively.

Figure 2. Time series of PM_1 species (Org, SO_4, NO_3, NH_4, Chl, K, KCl, and BC) and meteorological variables (wind direction (100 m) and wind speed (8 m)) during three firework events, i.e., (a) Lunar New Year, (b) Lunar Fifth Day, and (c) Lantern Festival. The two blue arrow lines represent the starting and ending times of fireworks events.

Figure 3. Correlation of PM_1 vs. $PM_{2.5}$ with the data segregated into three fireworks events (LNY, LFD, and LF) and non-fireworks periods (NFW). The blank circles represent FW data between 18:00 – 23:30 on 9 February which had large influences from NFW sources.

Figure 4. Average chemical composition of PM_1 and OA from fireworks and background during three FW events.

Figure 5. (a) Average mass spectra (MS) of OA during the firework period of Lunar New Year (23:30, 9 February – 3:30, 10 February) and the period of background (BG, 4:30 – 11:00, 10 February). (b) Comparison of the difference spectrum from (a), i.e., $MS_{FW+BG} - MS_{BG}$, with the average LV-OOA spectrum in Ng et al.(2011a). Note that five *m/z*'s, 37 ($^{37}Cl^+$), 58 ($NaCl^+$), 60 ($Na^{37}Cl^+$), 74 (KCl^+), and 76 ($K^{37}Cl^+$/ $^{41}KCl^+$) marked in the figure were dominantly from fragmentation of inorganic salts during fireworks.

Figure 6. Box plots of (a) mass concentrations and (b) mass fractions of aerosol species for 9 pollution events marked in Fig. 1. The mean (cross), median (horizontal line), 25th and 75th percentiles (lower and upper box), and 10th and 90th percentiles (lower and upper whiskers) are shown for each box.

Figure 7. Left panel: variations of chemical composition of (a) organics, SNA (=sulfate + nitrate + ammonium), and others (the rest species in PM_1); (b) SPM and PPM; and (c) SOA and POA as a function of PM_1 and organics loadings, respectively.

The middle and right panels show the diurnal profiles of composition and mass concentrations, respectively.

Figure 8. (a) Average mass fraction of organics (f_{Org}) as a function of PM_1 mass, and (b) correlations of extinction coefficients ($PM_{2.5}$) vs. PM_1 for 9 pollution events (PEs) and 9 clean periods (CPs) marked in Fig. 1. The error bar represents one standard deviations of the average for each event.

Figure 9. The average ratios of aerosol species, gaseous species, PM mass concentrations, extinction coefficient, and meteorological parameters between holiday (HD) and non-holiday (NHD) periods. Two different holidays, i.e., the official holiday of 9 – 15 February and the longer holiday of 7 – 20 February were used for averages. Also note that the averages were made by excluding clean periods and firework events during both HD and NHD days. The error bars are the standard errors of the ratios.

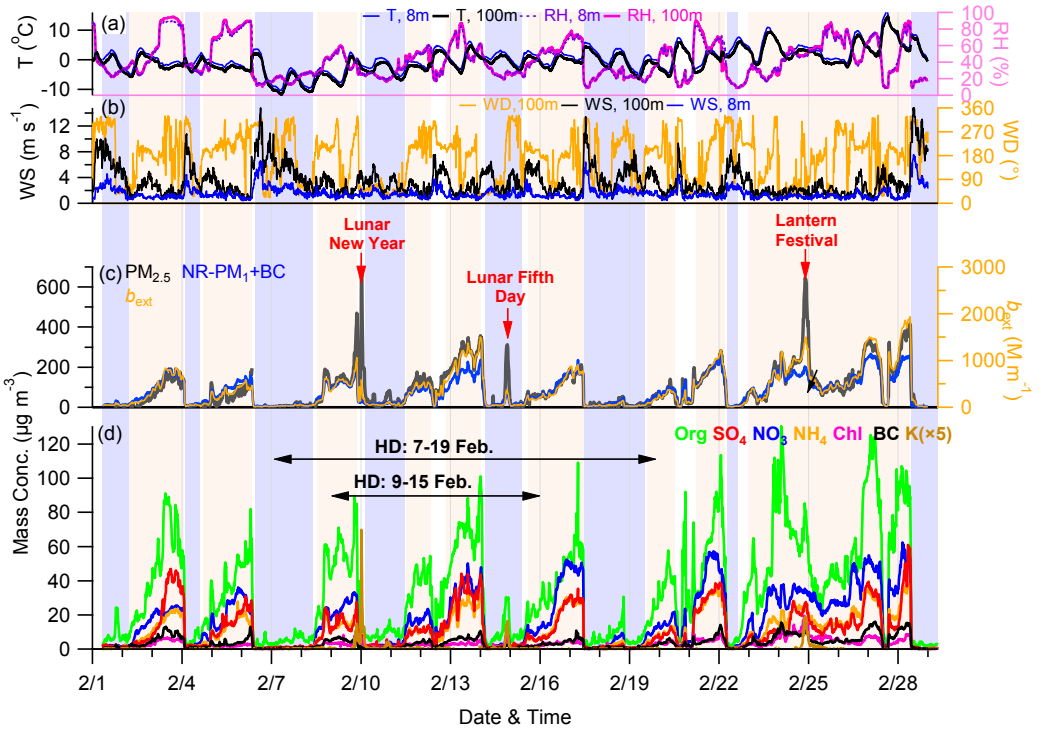

Figure 1. Time series of meteorological parameters (a) relative humidity (RH) and temperature (T); (b) wind direction (WD) and wind speed (WS) at the height of 8m and 100 m; mass concentrations of (c) $PM_{2.5}$ and NR-PM_1 + BC and (d) submicron aerosol species. The extinction coefficient (b_{ext}) at 630 nm is shown in (c). Three events, i.e., Lunar New Year (LNY), Lunar Fifth Day (LFD) and Lantern Festival (LF) with significant influences of fireworks are marked in (c). In addition, the classified clean periods (CPs) and polluted events (PEs) are marked as shaded light blue and pink areas, respectively.

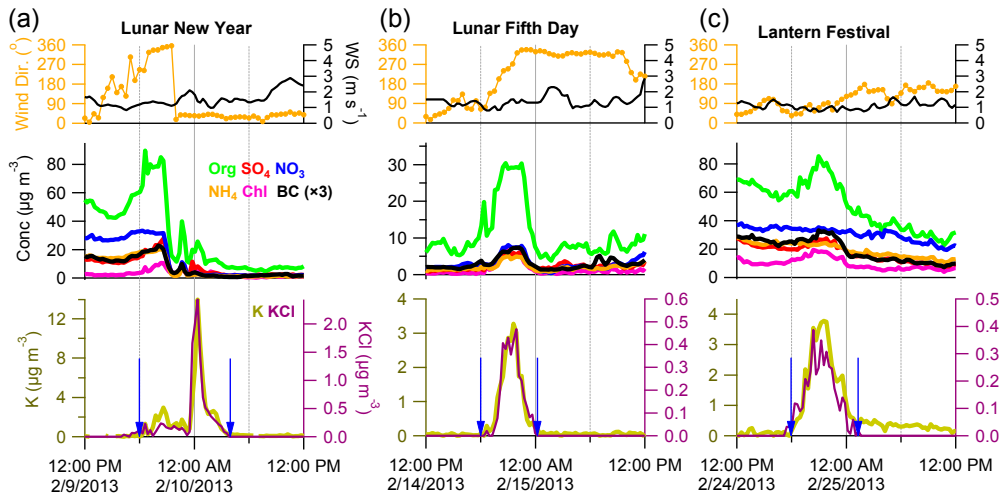

863

864 **Figure 2.** Time series of PM_1 species (Org, SO_4, NO_3, NH_4, Chl, K, KCl, and BC) and
865 meteorological variables (wind direction (100 m) and wind speed (8 m)) during three
866 firework events, i.e., (a) Lunar New Year, (b) Lunar Fifth Day, and (c) Lantern
867 Festival. The two blue arrow lines represent the starting and ending times of fireworks
868 events.

869

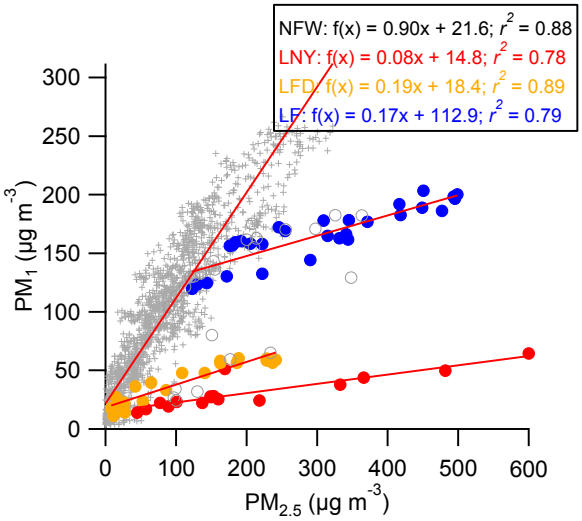

870

871 **Figure 3.** Correlation of PM_1 vs. $PM_{2.5}$ with the data segregated into three fireworks
872 events (LNY, LFD, and LF) and non-fireworks periods (NFW). The blank circles
873 represent FW data between 18:00 – 23:30 on 9 February which had large influences
874 from NFW sources.

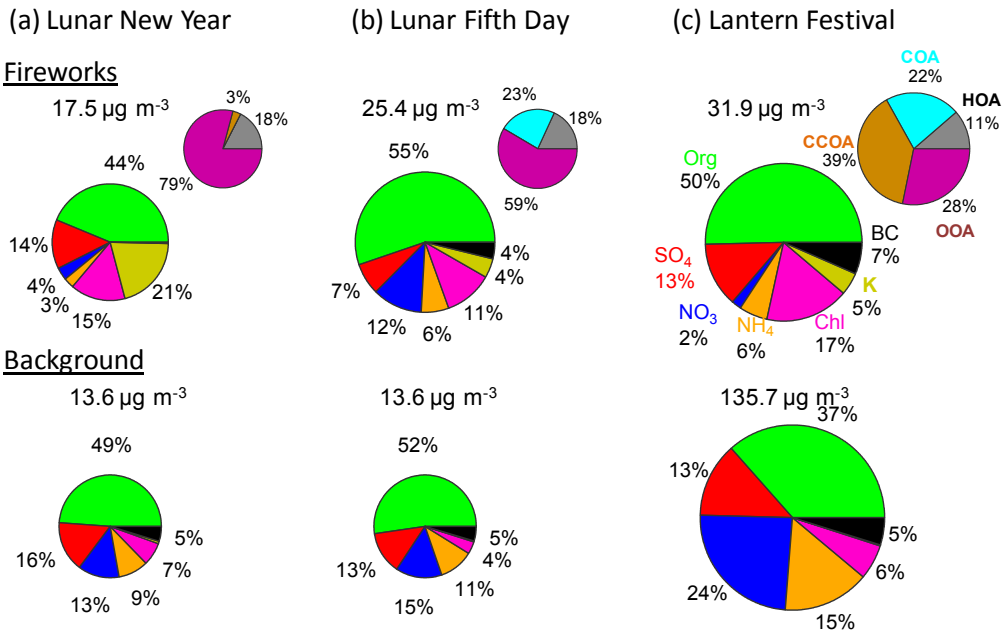

875

876 **Figure 4.** Average chemical composition of PM_1 and OA from fireworks and
877 background during three FW events.

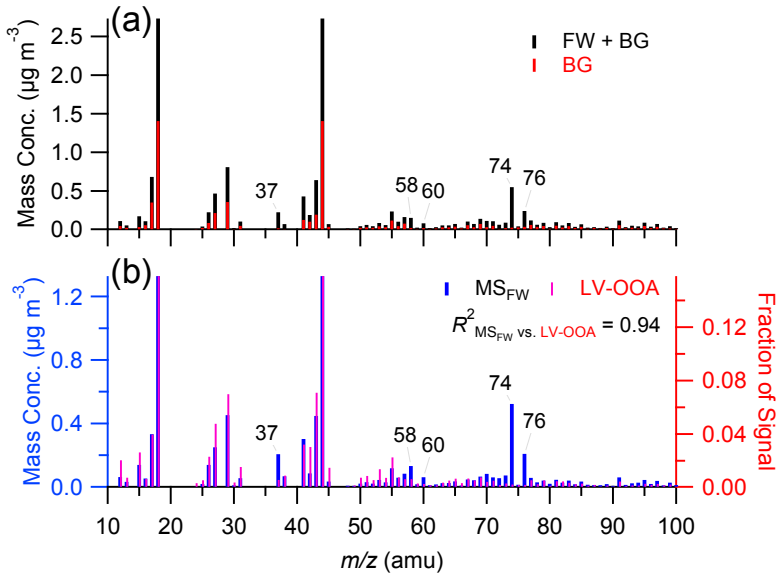

878

879 **Figure 5.** (a) Average mass spectra (MS) of OA during the firework period of Lunar
880 New Year (23:30, 9 February – 3:30, 10 February) and the period of background (BG,
881 4:30 – 11:00, 10 February). (b) Comparison of the difference spectrum from (a), i.e.,
882 $MS_{FW+BG} - MS_{BG}$, with the average LV-OOA spectrum in Ng et al.(2011a). Note that
883 five *m/z*'s, 37 ($^{37}Cl^+$), 58 ($NaCl^+$), 60 ($Na^{37}Cl^+$), 74 (KCl^+), and 76 ($K^{37}Cl^+$/ $^{41}KCl^+$)
884 marked in the figure were dominantly from fragmentation of inorganic salts during
885 fireworks.

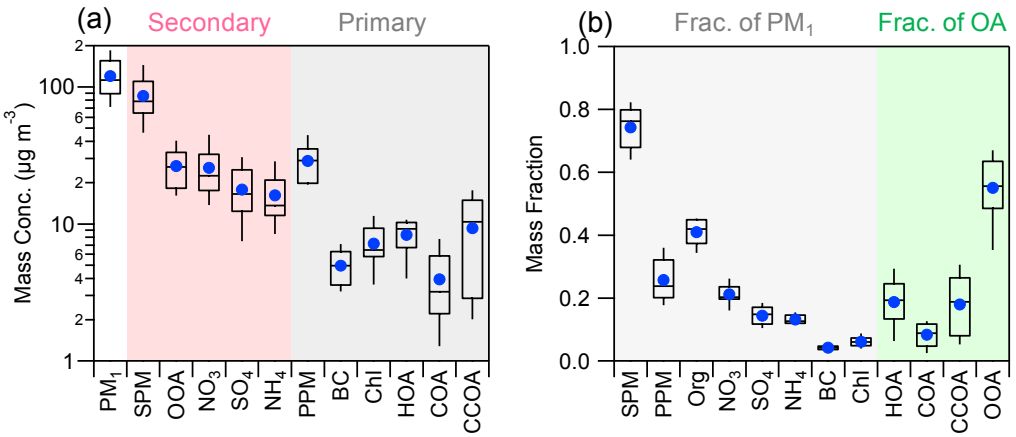

886

887 **Figure 6.** Box plots of (a) mass concentrations and (b) mass fractions of aerosol
888 species for 9 pollution events marked in Fig. 1. The mean (cross), median (horizontal
889 line), 25th and 75th percentiles (lower and upper box), and 10th and 90th percentiles
890 (lower and upper whiskers) are shown for each box.

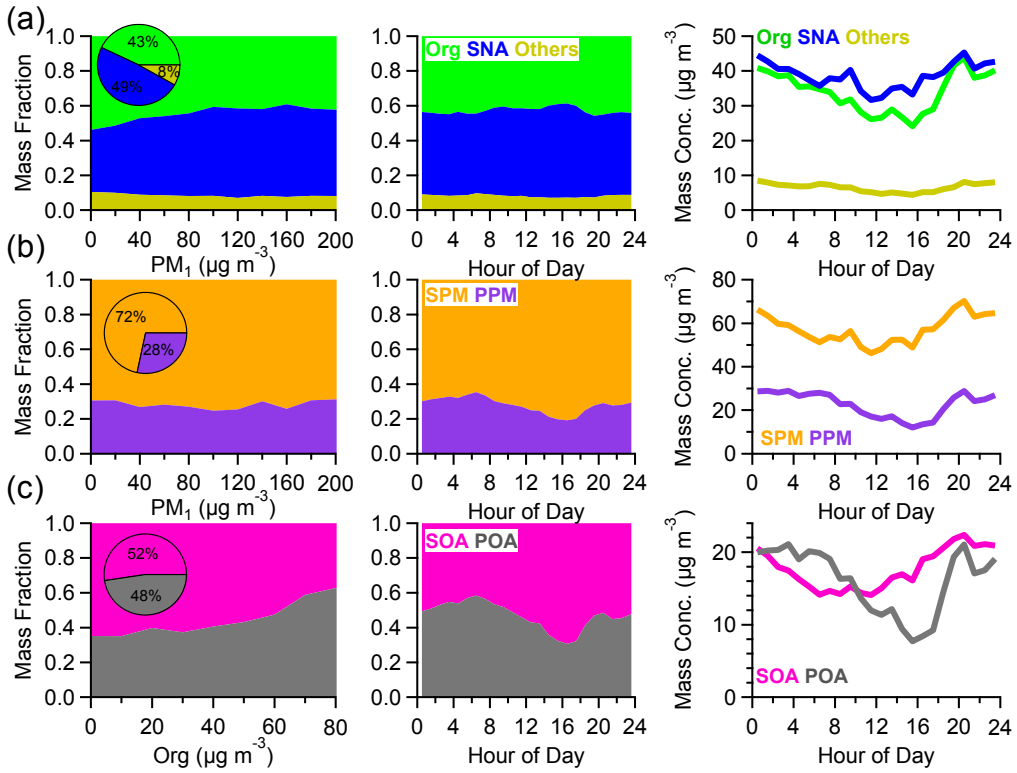

Figure 7. Left panel: variations of chemical composition of (a) organics, SNA (=sulfate + nitrate + ammonium), and others (the rest species in PM_1); (b) SPM and PPM; and (c) SOA and POA as a function of PM_1 and organics loadings, respectively. The middle and right panels show the diurnal profiles of composition and mass concentrations, respectively.

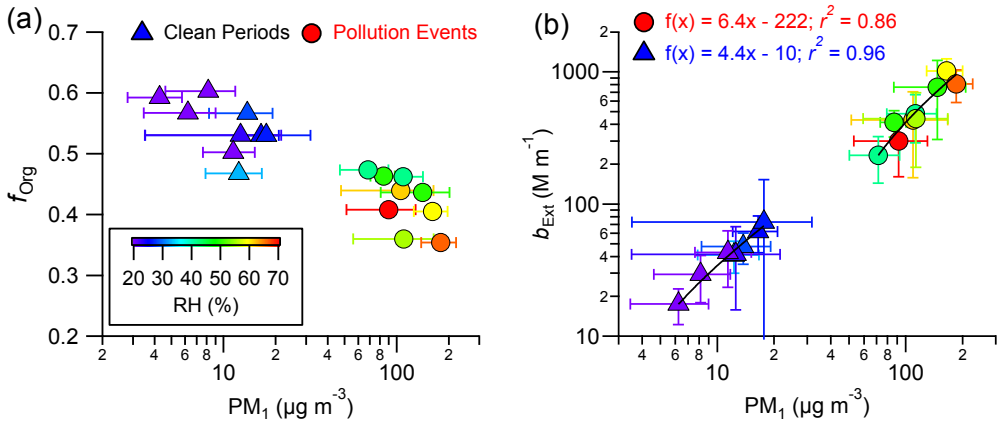

898

899 **Figure 8.** (a) Average mass fraction of organics (f_{Org}) as a function of PM_1 mass, and
900 (b) correlations of extinction coefficients ($PM_{2.5}$) vs. PM_1 for 9 pollution events (PEs)
901 and 9 clean periods (CPs) marked in Fig. 1. The error bar represents one standard
902 deviations of the average for each event.

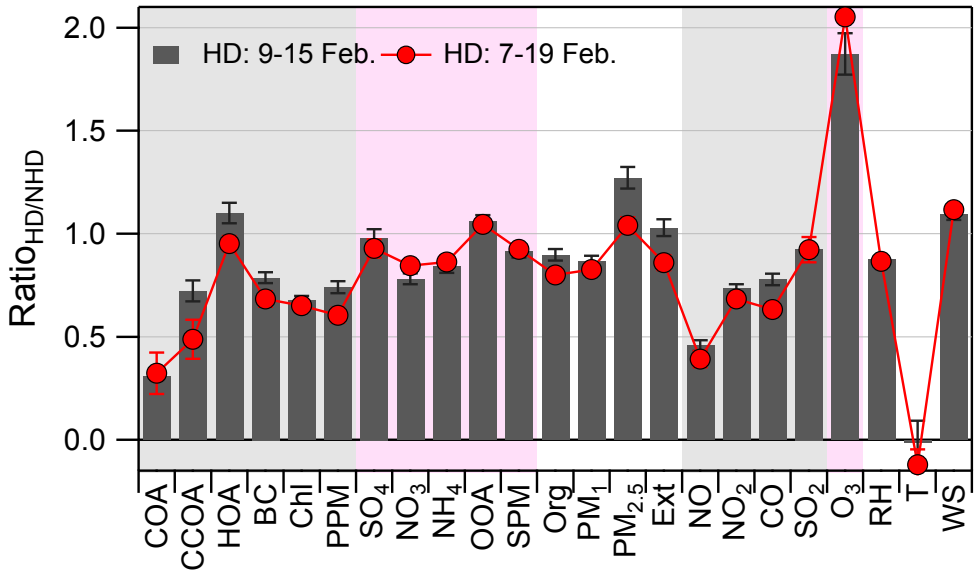

903

904 **Figure 9.** The average ratios of aerosol species, gaseous species, PM mass
905 concentrations, extinction coefficient, and meteorological parameters between holiday
906 (HD) and non-holiday (NHD) periods. Two different holidays, i.e., the official
907 holiday of 9 – 15 February and the longer holiday of 7 – 20 February were used for
908 averages. Also note that the averages were made by excluding clean periods and
909 firework events during both HD and NHD days. The error bars are the standard errors
910 of the ratios.